Universal scaling of plasmon coupling in metal nanostructures: Checking the validity for higher plasmonic modes using second harmonic generation

Jérémy Butet,[1,2,*] Isabelle Russier-Antoine,[2] Christian Jonin,[2] Noëlle Lascoux,[2] Emmanuel Benichou,[2] Olivier J. F. Martin,[1] and Pierre-François Brevet[2,†]

[1]*Nanophotonics and Metrology Laboratory (NAM), Swiss Federal Institute of Technology Lausanne (EPFL), 1015 Lausanne, Switzerland*
[2]*Institut Lumière Matière, Université Claude Bernard Lyon 1, CNRS, UMR5306, Université de Lyon, 69622 Villeurbanne Cedex, France*

(Received 26 March 2013; revised manuscript received 9 June 2013; published 28 June 2013)

The universal scaling of plasmon coupling in metallic nanostructures is now a well-established feature. However, if the interaction between dipolar plasmon modes has been intensively studied, this is not the case of the coupling between higher order ones. Using Mie theory extended to second harmonic generation, we investigate the coupling between quadrupolar plasmon modes in metallic nanoshells. Like in the case of dipolar plasmon modes, a universal scaling behavior is observed in agreement with the plasmon hybridization model.

DOI: 10.1103/PhysRevB.87.235437 PACS number(s): 78.67.Bf, 42.65.Ky, 73.20.Mf

I. INTRODUCTION

Metallic nanoparticles exhibit surface plasmon resonances corresponding to the collective excitation of their conduction electrons. These resonances lead to unique optical properties. The physical properties of these resonances, i.e., their energy and width, depend on the size, the shape, the morphology, or the chemical composition of the metallic nanostructure as well as their environment.[1] Strongly coupled collections of metallic nanostructures are of great interest in this context. They offer a wide range of possibilities to tailor the optical properties for specific practical applications.[2] The simplest example of plasmon coupling is the case of two nanoparticles placed very close to each other and forming a nanodimer.[3,4] The optical properties of nanodimers are very different from those of well-separated nanoparticles and strongly depend on the distance between the two nanoparticles.[3–5] Metallic nanoshells, effectively nanostructures composed of a dielectric core inside a metallic shell, are also simple examples of nanostructures in which plasmon coupling arises.[6] In comparison with the plasmon resonances of solid nanospheres, the plasmon resonance energy of a metallic nanoshell is highly tunable and can be controlled by modifying the core dielectric constant[7,8] or the shell thickness.[9] To describe such strongly coupled plasmonic systems, Nordlander and co-workers have introduced an analytical model that provides an intuitive picture of the coupling mechanisms in complex nanostructures.[10] In this hybridization model, the plasmon modes of complex nanostructures result from the interaction between the plasmon modes of their constituting elements. This elegant model has been successfully used to describe plasmon resonances in nanoshells,[10] concentric nanoshells,[10,11] gold nanostars,[12] nanoparticle dimers,[13] or plasmonic oligomers.[14,15]

In parallel to the hybridization model, it has been observed that the strength of the plasmon coupling between a pair of metallic nanoparticles decreases almost exponentially with the gap of nanometer dimension divided by the nanoparticle size.[16] This universal scaling of the plasmon coupling is independent of the nanoparticle size, shape, or metal nature.[16–18] The universal scaling of the plasmon coupling has also been reported for metallic nanoshells.[19] However, contrary to the case of nanoparticle dimers,[13] the plasmonic coupling in metallic nanoshells preserves the spherical symmetry of the problem under study. For this reason, the interaction can only occur between plasmonic modes with identical symmetry properties, i.e., with the same multipolar order, resulting in pure dipole-dipole or quadrupole-quadrupole interactions, and so on for higher order modes.[10] Therefore, plasmonic nanoshells are ideal systems for the study of plasmon coupling without interaction between modes with different order. Although the interaction between dipolar plasmon modes has been extensively discussed in the litterature,[10,11] this is not the case for higher plasmon modes such as the quadrupolar mode, for example. This lack stems, in particular, from the difficulty in observing higher plasmon modes using linear optics.

Nonlinear plasmonics, namely, the study of nonlinear optical processes in metal nanostructures, is a fast growing research field.[20] Second harmonic generation (SHG), the process whereby two photons at the fundamental frequency are converted into one photon at the second harmonic (SH) frequency, is one of the most studied nonlinear optical processes in plasmonic nanostructures.[21–28] Indeed, SHG is forbidden in centrosymmetric media within the dipolar approximation. This rule therefore considerably limits the SHG efficiency in cubic metals such as gold or silver. It, however, opens new routes for the study of plasmonic systems where surfaces play a major role. As an example, SHG was recently proposed for the investigation of nanosize defects in metallic nanostructures, demonstrating a much better sensitivity than linear optical processes.[29,30] It was further shown that SHG can also effectively increase the efficiency of plasmonic nanosensors.[31] This last property is based on the enhancement of the SHG intensity by surface plasmon resonances. SHG was also used for the characterization of the surface plasmons themselves, for instance, their dephasing time.[32]

In this paper, we investigate theoretically the universal scaling of plasmon coupling in metal nanostructures, with special attention paid to higher plasmon modes. Using Mie theory for metallic nanoshells and its extension to the SHG process,[33,34] the linear and nonlinear optical properties of plasmonic nanoshells are compared. It is emphasized, in particular, that SHG allows a straightforward observation of the quadrupolar plasmon resonance. As previously observed for the dipolar plasmon resonance, the quadrupolar plasmon resonance wavelength varies almost exponentially as the shell

thickness decreases. Furthermore, the wavelength shift of the quadrupolar plasmon resonance normalized by the solid sphere quadrupolar plasmon resonance wavelength depends on the shell thickness to core radius ratio and is independent of the nanoshell diameter. These results clearly demonstrate that the coupling between the quadrupolar plasmon modes follows a universal scaling law similarly to the dipolar plasmon mode.[19]

II. THEORETICAL METHODS

In this work, Mie theory is used to calculate both the linear extinction and the SH scattering cross sections of perfectly spherical nanoparticles, i.e., nanoshells.[33] Mie theory extended to SHG from nanoshells is briefly described in the present paper but all calculation details can be found elsewhere.[33] The first step of the nonlinear Mie theory is to expand the fundamental electric field of the exciting plane wave on the vector spherical harmonics basis. The coefficients of the expansion are found applying the boundary conditions at both the core-shell and shell-embedding medium interfaces. Note that the incident wave is assumed to be a plane wave in the present work. The dielectric constants for gold are taken from the literature.[35] The SH nonlinear polarization standing at both interfaces is then calculated considering a pure surface contribution. Indeed, SHG is forbidden in centrosymmetric media in the dipolar approximation, while the centrosymmetry is locally broken at the interface between two centrosymmetric media allowing for SHG. Only the $\chi^{(2)}_{\perp\perp\perp}$ component is retained, where the symbol $\perp$ denotes the direction normal to the interface. This tensor element is known to be the largest element of the surface susceptibility tensor in the case of metallic interfaces. For completeness, one would also need to incorporate other surface tensor elements and the bulk contribution which may turn out to be important for larger particles.[36,37] However, the energy or wavelength of the different plasmon modes enhancement of the SHG intensity would remain identical to the one observed for the single $\chi^{(2)}_{\perp\perp\perp}$ component. The scattered SH electric field in the far field is then obtained by applying the boundary conditions at both interfaces. The total SH scattering cross section is then given by

$$C_{\mathrm{sca}}(2\omega) = \frac{c}{8\pi k^2(2\omega)} \sum_{l,m}^{\infty} \left| A^{E,\mathrm{sca}}_{l,m}(2\omega) \right|^2, \qquad (1)$$

where the $A^{E,\mathrm{sca}}_{l,m}(2\omega)$ coefficients are the scattering coefficients weighting the contribution of the modes (l,m) to the total scattered wave. In this framework, the contribution of each emission mode is easily determined from the multipolar expansion.[33] As examples, the weight of the dipolar and quadrupolar modes in the SH scattered wave is calculated separately fixing $l = 1$ and $l = 2$, respectively. As a consequence, nonlinear Mie theory is perfectly suitable for the study of the coupling between higher plasmonic modes in metallic nanoshells.

III. RESULTS AND DISCUSSION

A. Linear optical properties of gold nanoshells

Figure 1(a) shows the linear extinction cross section as a function of the wavelength calculated for a 80 nm diameter

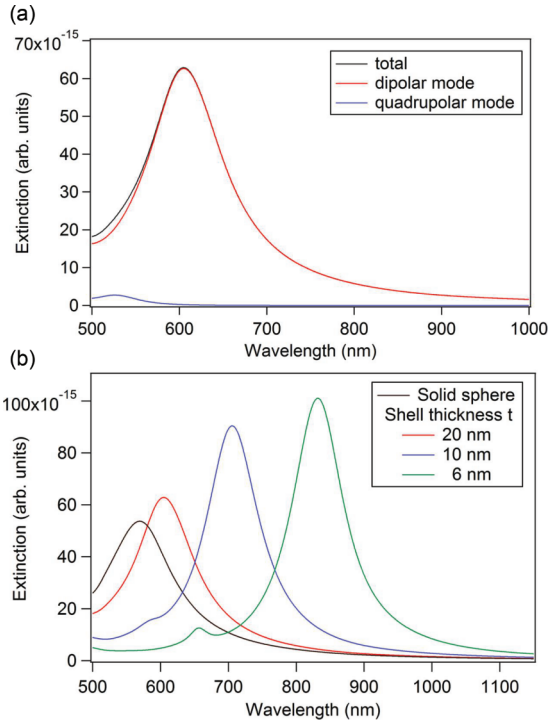

FIG. 1. (Color online) (a) Extinction spectrum for a silica core-gold shell nanoparticle (diameter $d = 100$ nm; shell thickness $t = 20$ nm) in water ($n = 1.33$) calculated using Mie theory and the dielectric constant of gold published in Ref. 35. The extinction cross section for the first two surface plasmon resonance modes is also shown, namely, the dipolar ($l = 1$) and the quadrupolar ($l = 2$) modes. (b) Extinction spectra for a 100 nm diameter gold solid sphere and 100 nm diameter silica core-gold shell nanoparticles in water ($n = 1.33$) calculated for different shell thicknesses ($t = 6$, 10, and 20 nm).

silica core covered with a gold nanoshell with a shell thickness $t = 20$ nm. The bulk dielectric constants of gold have been taken from experimental data.[35] The impact of the shell thickness on the gold dielectric constant, namely, the increased electron scattering at the shell boundaries, is taken into account although this correction barely modifies the plasmon resonance energy.[38] The extinction spectrum can be taken as the superposition of the first two contributing modes: the $l = 1$ dipolar and the $l = 2$ quadrupolar modes. The extinction spectrum thus possesses two resonances: a broad dipolar resonance close to 600 nm and a quadrupolar resonance close to 550 nm [see Fig. 1(a)]. Within the hybridization framework, the observed dipolar (respectively, quadrupolar) resonance corresponds to the symmetric coupling between the original dipolar (respectively, quadrupolar) plasmon modes of the gold sphere and that of the gold nanocavity, the two forming the nanoshell. The antisymmetric coupled plasmon modes do not contribute to the extinction spectrum since they weakly interact with an incident plane wave. For this reason, these modes are often referred to as optical dark modes. The mode resonances of the antisymmetric coupled plasmon modes occur at higher energies (i.e., shorter wavelengths) than that of the original uncoupled plasmon modes and the resonances of the symmetric coupled plasmon modes occur at lower energy (i.e., longer wavelengths) than that of the original uncoupled plasmon modes.[10] Furthermore, the

shell thickness has a great impact on these plasmon modes. Indeed, the coupling strength between the original sphere and the core plasmon modes dramatically depends on this geometric parameter:[10] the larger the shell thickness, the smaller the coupling between the original plasmon modes. As the coupling between the original plasmon modes increases, the mode energy of the antisymmetric coupled plasmon modes increases (i.e., the mode is blueshifted) and the mode energy of the symmetric coupled modes decreases (i.e., the mode is redshifted). Figure 1(b) shows the extinction cross section calculated for a 100 nm diameter solid sphere and for a 100 nm diameter silica core-gold shell nanoparticle with different shell thicknesses ($t = 6$, 10, and 20 nm). All spectra are dominated by the dipolar plasmon resonance which shifts from $\lambda_0 = 570$ nm for the solid sphere to 832 nm for a 6 nm shell thickness. The quadrupolar resonance is observed for shell thicknesses t below or equal to 10 nm but its amplitude in this case is much smaller than the amplitude of the dipolar plasmon resonance. Higher plasmon resonances have been experimentally observed in the case of nanoshells, though for very high shell thicknesses to outer diameter ratios, i.e., strong plasmon coupling.[6,39] The quadrupolar resonance observed in the extinction spectrum of the 100 nm diameter silica core-gold shell nanoparticle with a shell thickness $t = 6$ nm corresponds to an enhancement of the absorption cross section and therefore cannot be observed with dark-field microscopy, for instance, where only scattering is involved. This feature emphasizes why linear optics is not well suited for the characterization of higher order plasmon modes. Hence, SHG was recently proposed as an interesting alternative to linear optics for the monitoring of higher plasmonic modes.[31] The SH quadrupolar emission from spherical metallic nanoparticles has indeed been observed at the single nanoparticle level.[28,29] Furthermore, polarization resolved hyper-Rayleigh scattering has been shown to allow for a straightforward separation between even and odd mode contributions to the SH scattered wave.[40,41]

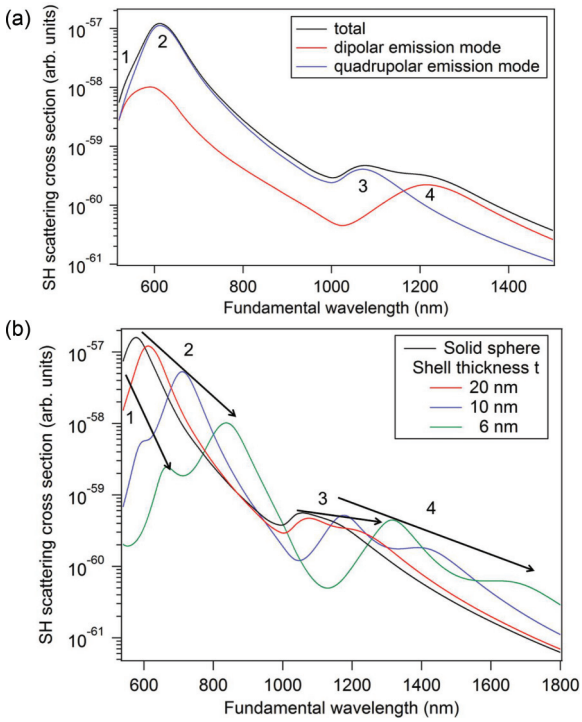

FIG. 2. (Color online) (a) SH scattering cross section for a silica core-gold shell nanoparticle (diameter $d = 100$ nm; shell thickness $t = 20$ nm) in water ($n = 1.33$) calculated with the extended Mie theory using the dielectric constant of gold published in Ref. 35. The contributions of the first two SH emission modes are shown, namely, the dipolar (red curve) and quadrupolar modes (blue curve). The labeled resonances correspond to those discussed in the main text. (b) SH scattering cross section for a 100 nm diameter gold solid sphere and 100 nm diameter silica core-gold shell nanoparticles in water ($n = 1.33$) calculated for different shell thicknesses ($t = 6$, 10, and 20 nm). The arrows indicate the wavelength shift of the different resonances when the shell thickness decreases.

B. Second harmonic generation from gold nanoshells

By using Mie theory extended to the SHG to describe plasmonic nanoshells,[33,34] the SH scattering cross section was calculated for a 100 nm diameter silica core-gold shell nanoparticle with a $t = 20$ nm shell thickness and the contributions of the SH dipolar ($l = 1$) and quadrupolar ($l = 2$) emission modes were easily separated [see Fig. 2(a)]. The corresponding extinction spectrum is shown in Fig. 1(a). The SHG spectrum reveals four surface plasmon resonances corresponding to the enhancement of the SH dipolar emission mode, the SH quadrupolar emission mode, or to the enhancement of both emission modes. As discussed by Dadap *et al.* in his seminal work,[42] the most efficient mechanism leading to the SH dipolar emission mode from spherical nanostructures is the $E_1 + E_2 \rightarrow E_1$ mechanism where the terms on the left side of the arrow refer to the nature of the nanosphere interaction with the fundamental wave and the term on the right side describes the SH emission mode. Hence, this notation describes here a dipolar emission (E_1) driven by the combination of an electric dipole (E_1) and an electric quadrupole (E_2) excitation at the fundamental wavelength. The pure dipolar mode $E_1 + E_1 \rightarrow E_1$ mechanism is here forbidden since nanoshells are centrosymmetric spherical nano-objects. The SH dipolar emission indeed needs retardation in the electromagnetic excitation at the fundamental frequency, a requirement fulfilled through the quadrupolar mode in the lowest order approximation. On the contrary, the quadrupolar SH emission mode can be excited without retardation at the fundamental frequency and arises from the $E_1 + E_1 \rightarrow E_2$ mechanism. The resonances labeled 3 and 4 in Fig. 2(a) are the symmetric quadrupolar and the symmetric dipolar plasmon resonances, respectively.[33] In this case, only the emission mode with symmetry properties identical to the surface plasmon resonance is enhanced, e.g., only the SH dipolar (respectively, quadrupolar) emission mode is enhanced when the SH frequency is tuned close to the symmetric dipolar (respectively, quadrupolar) surface plasmon resonance. Both the dipolar and the quadrupolar emission modes are enhanced at resonances 1 and 2. In the latter cases, the fundamental wavelength is tuned close to the dipolar and quadrupolar resonances and both emission modes take advantage of the enhanced electric field at the fundamental frequency.

As previously discussed, SHG from metallic nanoshells is enhanced by surface plasmon resonances, the energy of which depends on the shell thickness.[10,43] Figure 2(b) shows the SH cross section calculated for a 100 nm diameter gold

solid sphere and a 100 nm diameter silica core-gold shell nanoparticle in a water background ($n = 1.33$) with different shell thicknesses ($t = 6$, 10, and 20 nm). Like in the linear extinction spectra, all the resonances are redshifted as the shell thickness decreases. Furthermore, the maximum of the resonance labeled 3 (respectively, 4) occurs at a wavelength exactly twice the wavelength at which occurs the resonances labeled 1 (respectively, 2). This result is expected and underlines the robustness of our computations. Furthermore, this result unambiguously demonstrates that SHG is suitable for the investigation of the universal scaling law of plasmon coupling in metal nanostructures. In the following, we will only consider the case of the SHG enhancement by surface plasmon resonances at the SH wavelength. This configuration is often experimentally preferred in order to prevent any nanostructure damages. Moreover, the role played by each plasmon resonance is well defined since only the SH dipolar (respectively, quadrupolar) emission mode is enhanced by the dipolar (respectively, quadrupolar) plasmon resonance.[33,42]

C. Impact of the diameter and shell thickness

Computations were performed for different outer diameters ($d = 60$, 80, 100, and 120 nm). The wavelength maximum of the SH dipolar (respectively, quadrupolar) emission modes are shown as a function of the shell thickness t in Fig. 3(a) [respectively, Fig. 3(b)]. For both emission modes and for all diameters, almost single exponential decays are observed as a function of the shell thickness. The data were fitted with the equation $y = y_0 + \alpha \exp(-t/\beta)$, where y_0, α, and β are three free parameters.[19] For the SH dipolar emission mode, the best agreement is found for $\beta = 4.11 \pm 0.20$ nm, 4.75 ± 0.23 nm, 5.49 ± 0.26 nm, and 5.77 ± 0.39 nm for the respective nanoshell diameters $d = 60$, 80, 100, and 120 nm. These values are in agreement with those reported by Jain *et al.* for the dipolar plasmon resonance.[15] In the case of the SH quadrupolar emission mode, the best agreement is found for $\beta = 3.39 \pm 0.08$ nm, 4.09 ± 0.17 nm, 4.52 ± 0.21 nm, and 4.99 ± 0.25 nm for the respective nanoshell diameters $d = 60$, 80, 100, and 120 nm. For all diameters, the value of β is smaller for the SH quadrupolar emission mode than for the SH dipolar emission mode. This behavior is well explained by the hybridization model introduced by Prodan *et al.*[10,43] The nanoshell plasmon modes arise from the coupling of the original cavity plasmon modes with the sphere plasmon modes.[10] Furthermore, only plasmon modes with identical symmetry properties effectively interact.[43] For example, the dipolar (respectively, quadrupolar) nanocavity plasmon mode effectively interacts with the dipolar (respectively, quadrupolar) nanosphere plasmon mode. Using an incompressible fluid model for the description of the conduction electron displacement, it was also shown that the strength of the plasmon coupling in metallic nanoshells is proportional to the quantity $x^{l+1/2}$, where x is the aspect ratio of the shell (the inner radius divided by the outer radius) and l is the plasmon mode order.[43] Since the plasmon coupling strength depends on the mode order, different values of β are expected for the SH dipolar and quadrupolar emission modes. Furthermore, the hybridization model predicts that, for a given x ratio, the plasmon coupling strength decreases with the increasing plasmon mode order.[43] For this reason, the impact of the shell thickness on the plasmon resonance energy is larger for the dipolar mode than for the quadrupolar mode, explaining the higher value of β for the SH dipolar emission mode.

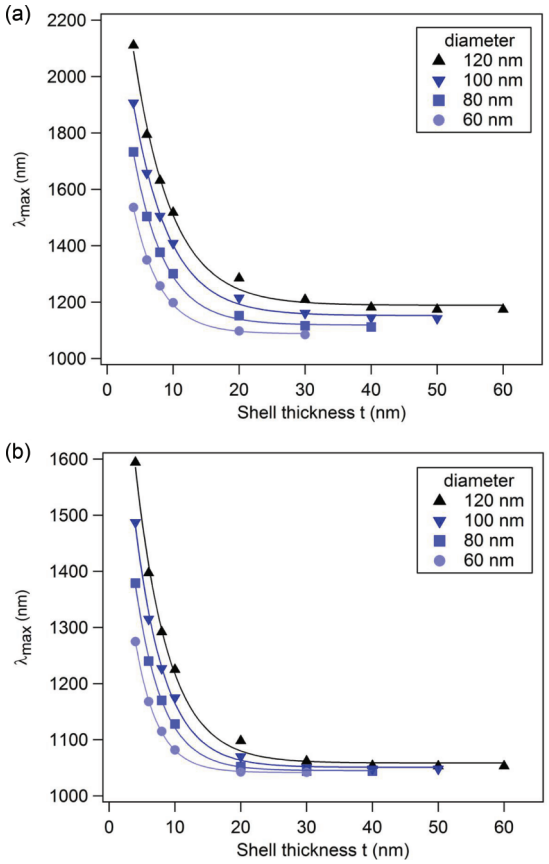

FIG. 3. (Color online) Calculated fundamental wavelength λ_{max} of the maximum of the SH (a) dipolar and (b) quadrupolar emission modes for a silica core-gold shell nanoparticle in water as a function of the shell thickness t for four nanoshell diameters. Solid lines correspond to fits with exponential functions.

D. Universal scaling of plasmon coupling

To proceed with the determination of the universal scaling of plasmon coupling between higher plasmon modes, the fractional shift $\Delta\lambda/\lambda_0$ of the SH dipolar and quadrupolar emission modes of a silica core-gold shell nanoparticle in water with respect to that of a solid gold nanosphere were plotted as a function of the shell thickness to the core radius ratio t/R for four different diameters in Fig. 4. For both the dipolar and the quadrupolar modes, almost exponential decays are observed. Both curves were fitted with the equation $y = \alpha \exp(-t/\gamma R)$.[19] For the SH dipolar mode, the best agreement is obtained for $\gamma = 0.159 \pm 0.008$. This value matches well that reported for the dipolar plasmon resonance monitored with linear optics.[19] The value obtained for the SH quadrupolar emission mode is smaller with a value of $\gamma = 0.125 \pm 0.007$. These results confirm that the coupling between higher order plasmon resonances follows a universal scaling behavior as was previously demonstrated for dipolar plasmon resonances. Furthermore, these results confirm that the plasmon coupling

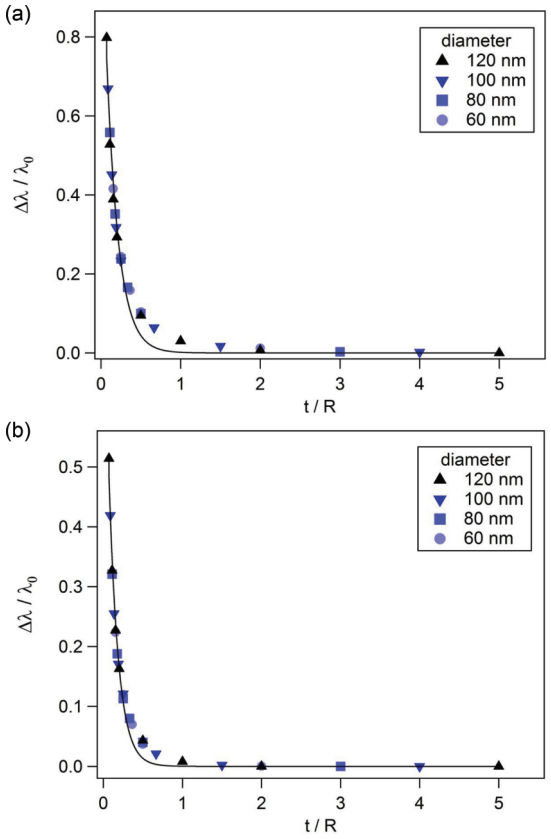

FIG. 4. (Color online) Fractional shift $\Delta\lambda/\lambda_0$ of the SH (a) dipolar and (b) quadrupolar emission modes for a silica core-gold shell nanoparticle in water with respect to that of a solid gold nanosphere with the same size, as a function of the ratio of the shell thickness to the core radius t/R for four different diameters. The solid lines correspond to fits with exponential functions.

strength decreases with the increasing plasmon order l. From the fit of the universal trend exhibited by the surface plasmon resonance energy, the following formula is obtained:

$$\frac{\Delta\lambda^{\mathrm{dip}}}{\lambda_0^{\mathrm{dip}}} = 0.81 \times e^{-(t/0.159R)} \tag{2}$$

for the wavelength of the SH dipolar emission mode, where λ_0^{dip} is the SH dipolar emission mode wavelength for a solid sphere with the same size as the nanoshell and $\Delta\lambda^{\mathrm{dip}} = \lambda_{\mathrm{max}}^{\mathrm{dip}} - \lambda_0^{\mathrm{dip}}$ is the wavelength shift of the nanoshell SH dipolar emission mode from the solid sphere SH dipolar emission mode. Similarly, the following formula is obtained:

$$\frac{\Delta\lambda^{\mathrm{quad}}}{\lambda_0^{\mathrm{quad}}} = 0.51 \times e^{-(t/0.125R)} \tag{3}$$

for the wavelength of the SH quadrupolar emission mode, where $\lambda_0^{\mathrm{quad}}$ is the SH quadrupolar emission mode wavelength for a solid sphere of the same size as the nanoshell and $\Delta\lambda^{\mathrm{quad}} = \lambda_{\mathrm{max}}^{\mathrm{quad}} - \lambda_0^{\mathrm{quad}}$ is the wavelength shift of the nanoshell SH quadrupolar emission mode from the solid sphere SH quadrupolar emission mode. Equation (2) slightly differs from the one reported by Jain *et al.*, which is $\Delta\lambda^{\mathrm{dip}}/\lambda_0^{\mathrm{dip}} = 0.97\exp(-t/0.18R)$.[19] Interestingly, the impact of the shell thickness on the gold dielectric constant is taken into account in the present work, whereas this was not the case in Ref. 19. Equations (2) and (3) allow for the determination of the SH dipolar and quadrupolar emission mode wavelengths which correspond to the symmetric dipolar and quadrupolar plasmon resonance modes. These results emphasize that plasmon scaling laws can indeed be derived for higher order plasmon modes, and in the case of the quadrupolar one, SHG is an adequate tool to observe it.[27]

IV. CONCLUSION

In summary, the universal scaling of plasmon coupling in metal nanostructures has been theoretically investigated using SHG with particular attention paid to higher order plasmon modes, beyond the dipolar case. As previously observed for the dipolar plasmon resonance, the quadrupolar plasmon resonance wavelength is found to vary exponentially with the shell thickness. Remarkably, the wavelength shift of the quadrupolar plasmon resonance scaled by the solid sphere quadrupolar plasmon resonance wavelength depends on the ratio of the shell thickness to the core radius and is independent of the nanoshell diameter. These results show, in the specific case of the quadrupolar mode, that the coupling between higher order plasmon modes also follows a universal scaling law similarly to that of dipolar plasmon modes. This work paves the way for the design of efficient nonlinear plasmonic nanorulers based on higher order plasmon modes.[5,44–46]

*jeremy.butet@epfl.ch
†pfbrevet@univ-lyon1.fr

[1] S. A. Maier, *Plasmonics: Fundamentals and Applications* (Springer, New York, 2007).
[2] N. J. Halas, S. Lal, W.-S. Chanq, S. Link, and P. Nordlander, Chem. Rev. **111**, 3913 (2011).
[3] K.-H. Su, Q.-H. Wei, X. Zhang, J. J. Mock, D. R. Smith, and S. Schultz, Nano Lett. **3**, 1087 (2003).
[4] T. Atay, J.-H. Song, and A. V. Nurmikko, Nano Lett. **4**, 1627 (2004).
[5] C. Sönnischen, B. M. Reinhard, J. Liphardt, and A. P. Alivisatos, Nat. Biotechnol. **23**, 741 (2005).
[6] S. J. Oldenburg, R. D. Averitt, S. L. Westcott, and N. J. Halas, Chem. Phys. Lett. **288**, 243 (1998).
[7] R. Bardhan, N. K. Grady, T. Ali, and N. J. Halas, ACS Nano **4**, 6169 (2010).
[8] E. Prodan, A. Lee, and P. Nordlander, Chem. Phys. Lett. **360**, 325 (2002).
[9] C. L. Nehl, N. K. Grady, G. P. Goodrich, F. Tam, N. J. Halas, and J. H. Hafner, Nano Lett. **4**, 2355 (2004).
[10] E. Prodan, C. Radloff, N. J. Halas, and P. Nordlander, Science **302**, 419 (2003).
[11] C. Radloff and N. J. Halas, Nano Lett. **4**, 1323 (2004).

[12]F. Hao, C. L. Nehl, J. H. Hafner, and P. Nordlander, Nano Lett. **7**, 729 (2007).
[13]P. Nordlander, C. Oubre, E. Prodan, K. Li, and M. I. Stockman, Nano Lett. **4**, 899 (2004).
[14]J. A. Fan, C. Wu, K. Bao, J. Bao, R. Bardhan, N. J. Halas, V. N. Manoharan, P. Nordlander, G. Shvets, and F. Capasso, Science **328**, 1135 (2010).
[15]M. Hentschel, M. Saliba, R. Vogelgesang, H. Giessen, A. P. Alivisatos, and N. Liu, Nano Lett. **10**, 2721 (2010).
[16]P. K. Jain, W. Huang, and M. A. El-Sayed, Nano Lett. **7**, 2080 (2007).
[17]K. C. Woo, L. Shao, H. Chen, Y. Liang, J. Wang, and H.-Q. Lin, ACS Nano **5**, 5976 (2011).
[18]M. D. Arnold, M. G. Blaber, M. J. Ford, and N. Harris, Opt. Express **18**, 7528 (2010).
[19]P. K. Jain and M. A. El-Sayed, Nano Lett. **7**, 2854 (2007).
[20]M. Kauranen and A. V. Zayats, Nat. Photonics **6**, 737 (2012).
[21]A. Bouhelier, M. Beversluis, A. Hartschuh, and L. Novotny, Phys. Rev. Lett. **90**, 013903 (2003).
[22]V. K. Valev, N. Smisdom, A. V. Silhanek, B. De Clercq, W. Gillijns, M. Ameloot, V. V. Moshchalkov, and T. Verbiest, Nano Lett. **9**, 3945 (2009).
[23]K. Thyagarajan, S. Rivier, A. Lovera, and O. J. F. Martin, Opt. Express **20**, 12860 (2012).
[24]J. Berthelot, G. Bachelier, M. Song, P. Rai, G. Colas des Francs, A. Dereux, and A. Bouhelier, Opt. Express **20**, 10498 (2012).
[25]Y. Zhang, N. K. Grady, C. Ayala-Orozco, and N. J. Halas, Nano Lett. **11**, 5519 (2011).
[26]J. Duboisset, I. Russier-Antoine, E. Benichou, G. Bachelier, Ch. Jonin, and P.-F. Brevet, J. Phys. Chem. C **113**, 13477 (2009).
[27]J. Butet, J. Duboisset, G. Bachelier, I. Russier-Antoine, E. Benichou, C. Jonin, and P.-F. Brevet, Nano Lett. **10**, 1717 (2010).
[28]B. K. Canfield, H. Husu, J. Laukkanen, B. F. Bai, M. Kuittinen, J. Turunen, and M. Kauranen, Nano Lett. **7**, 1251 (2007).
[29]G. Bautista, M. J. Huttunen, J. Mäkitalo, J. M. Kontio, J. Simonen, and M. Kauranen, Nano. Lett. **12**, 3207 (2012).
[30]J. Butet, K. Thyagarajan, and O. J. F. Martin, Nano Lett. **13**, 1787 (2013).
[31]J. Butet, I. Russier-Antoine, C. Jonin, N. Lascoux, E. Benichou, and P.-F. Brevet, Nano Lett. **12**, 1697 (2012).
[32]B. Lamprecht, A. Leitner, and F. R. Aussenegg, Appl. Phys. B **68**, 419 (1999).
[33]J. Butet, I. Russier-Antoine, C. Jonin, N. Lascoux, E. Benichou, and P.-F. Brevet, J. Opt. Soc. Am. B **29**, 2213 (2012).
[34]J. Butet, I. Russier-Antoine, C. Jonin, N. Lascoux, E. Benichou, and P.-F. Brevet, J. Phys. Chem. C **117**, 1172 (2012).
[35]P. B. Johnson and R. W. Christy, Phys. Rev. B **6**, 4370 (1972).
[36]F. X. Wang, F. J. Rodríguez, W. M. Albers, R. Ahorinta, J. E. Sipe, and M. Kauranen, Phys. Rev. B **80**, 233402 (2009).
[37]G. Bachelier, J. Butet, I. Russier-Antoine, C. Jonin, E. Benichou, and P.-F. Brevet, Phys. Rev. B **82**, 235403 (2010).
[38]R. D. Averitt, D. Sarkar, and N. J. Halas, Phys. Rev. Lett. **78**, 4217 (1997).
[39]S. J. Oldenburg, J. B. Jackson, S. L. Westcott, and N. J. Halas, Appl. Phys. Lett. **75**, 2897 (1999).
[40]E. C. Hao, G. C. Schatz, R. C. Johnson, and J. T. Hupp, J. Chem. Phys. **117**, 5963 (2002).
[41]J. Butet, G. Bachelier, I. Russier-Antoine, C. Jonin, E. Benichou, and P.-F. Brevet, Phys. Rev. Lett. **105**, 077401 (2010).
[42]J. I. Dadap, J. Shan, and T. F. Heinz, J. Opt. Soc. Am. B **21**, 1328 (2004).
[43]E. Prodan and P. Nordlander, J. Chem. Phys. **120**, 5444 (2004).
[44]R. T. Hill, J. J. Mock, A. Hucknall, S. D. Wolter, N. M. Jokerst, D. R. Smith, and A. Chilkoti, ACS Nano **6**, 9237 (2012).
[45]B. Gallinet, T. Siegfried, H. Sigg, P. Nordlander, and O. J. F. Martin, Nano Lett. **13**, 497 (2013).
[46]N. Liu, M. Hentschel, T. Weiss, A. P. Alivisatos, and H. Giessen, Science **332**, 1407 (2011).